Intrinsic Reactivity of Gaseous Halocarbocations toward Model Aromatic Compounds

Ana E. P. M. Sorrilha,[†] Leonardo S. Santos,[†] Fábio C. Gozzo,[†] Regina Sparrapan,[†] Rodinei Augusti,*[,‡] and Marcos N. Eberlin*[,†]

Institute of Chemistry, State University of Campinas (UNICAMP), 13083-970 Campinas, SP Brazil, and Department of Chemistry, Federal University of Minas Gerais (UFMG), 31270-901 Belo Horizonte, MG Brazil

Received: March 12, 2004; In Final Form: May 11, 2004

The gas-phase reactivity of a set of halocarbocations, $^{+}CH_2X$ (X = Cl, Br, or I), $^{+}CHX^1X^2$ (X^1, X^2 = F, Cl, or Br), and $^{+}CX_3$ (X = F or Cl), with four prototype aromatic compounds (benzene, furan, pyrrole, and pyridine) was investigated via double- and triple-stage mass spectrometry and compared to that of the simplest $^{+}CH_3$ carbocation. A rich chemistry is observed, and the reaction channels are greatly influenced by the number and type of halogen substituents (X), the strength of the C−X bonds, the nature of the aromatic compound, and the relative stabilities of the carbocation products. $[Ar-CH_2]^+$, $[Ar-CHX]^+$, or $[Ar-CX^1X^2]^+$ functionalization of the relatively inert aromatic Ar−H bonds is the main reaction channel observed. A structure-specific "methylene by hydride exchange" reaction with toluene and B3LYP/6-311G(d,p) calculations indicate that the benzylium ion and the 2-furanylmethyl cation are formed in the $[Ar-CH_2]^+$ functionalization of benzene and furan, respectively. Kinetic isotope effects for the $[Ar-CHX]^+$ functionalization using naturally occurring halogen isotopes ($^{35}Cl/^{37}Cl$ and $^{79}Br/^{81}Br$) were measured. Using halogen-mixed halocarbocations $^{+}CHX^1X^2$, we evaluated the intrinsic competition for either the $[Ar-CHX^1]^+$ or $[Ar-CHX^2]^+$ functionalization. In reactions with pyridine, no Ar−H functionalization occurs and either proton transfer, N-addition, or net $[CH_2]^{+\bullet}$ transfer due to the loss of $X^\bullet$ from the nascent adducts is observed. Structural characterization of product ions was performed by on-line collision-induced dissociation or ion/molecule reactions, or both, and when possible by comparison with authentic ions.

Introduction

A century has now passed since Norris,[1] as well as Kehrmann and Wentzel,[2] recognized the first stable carbocation in solution: the triphenylmethyl cation $^{+}CPh_3$.[3] Since that time, general methods for preparing many persistent long-lived carbocations in the condensed phase have been developed, and the importance of carbocations in many chemical, industrial, and biological processes has been widely demonstrated. Carbocations are now fully recognized as key intermediates in innumerous reactions, many of which have industrial relevance.[3] Since the 1970s, mass spectrometric techniques have been used to form and to study the intrinsic reactivity and stability of gaseous long-lived stable carbocations, and relationships between condensed-phase and gas-phase reactivity have been established.[4]

In recent years, gaseous halogen-stabilized carbocations, the halocarbocations, have increasingly received attention. For instance, Cacace et al.[5] demonstrated that halocarbocations are possibly involved in important atmospheric processes. Hence, ionization of mixtures containing ozone and the CHX_2Y halogenated methanes (X = H, Cl, or F; Y = Cl or F) forms $[CHXY-O_3]^+$ adducts, which undergo unimolecular dissociation into $[HXYO_2]^+$ and CO (eq 1).

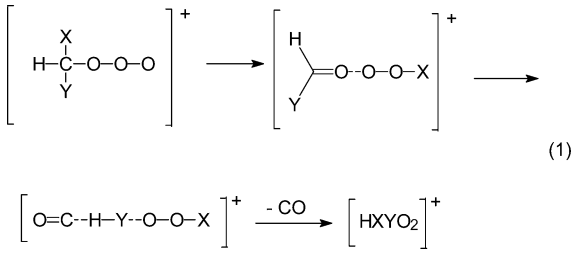

(1)

Eigendorf et al.[6] showed that the reactions of halocarbocations (Y^+), generated from halogenated hydrocarbons (CH_2Cl_2, $CHCl_3$, CCl_4, 1,1-dichloroethane, CH_2F_2, and 1,1-difluoroethane), with polycyclic aromatic hydrocarbons (PAHs) differentiate a series of structural isomers due to the formation of $[PAH + Y]^+$ and $[PAH + Y - H-X]^+$ products (X = Cl or F). The use of halomethanes leads predominantly to the elimination products $[PAH + Y - H-X]^+$, whereas haloethanes yield significant amounts of $[PAH + Y]^+$ adducts.

Cooks et al.[7] also showed that low-energy collisions of ionized halocarbenes with molecular oxygen lead to (i) decarbonation with the formation of the dihalogen molecular cation (eq 2) and (ii) oxygenolysis yielding XCO^+ (eq 3). Both

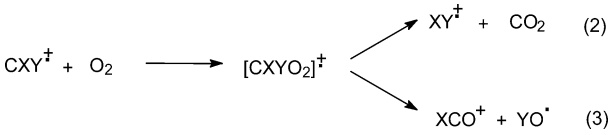

(2)

(3)

* To whom correspondence should be addressed.
[†] UNICAMP.
[‡] UFMG.

10.1021/jp0488822 CCC: $27.50
Published on Web 07/27/2004

TABLE 1: Main Products from the Gas-Phase Reaction between the Halocarbocations with the Four Prototype Aromatic Compounds

aromatic compound	product *m/z* (relative intensity, %)										
	$^+CH_3$	$^+CH_2Cl$	$^+CH_2Br$	$^+CH_2I$	$^+CHF_2$	$^+CHCl_2$	$^+CHBr_2$	^+CHClF	^+CHBrCl	$^+CCl_3$	$^+CF_3$
benzene	78 (100)	78 (8) 91 (100)	78 (32) 91 (100)	78 (63) 91 (100) 92 (18)	78 (28) 109 (100)	78 (18) 125 (100)	78 (23) 91 (14) 169 (100)	78 (38) 109 (100)	78 (24) 91 (3) 125 (100) 169 (18)	78 (1) 125 (14) 159 (100)	78 (100) 127 (21)
furan	68 (100)	68 (100) 81 (38)	68 (100) 81 (3)	68 (100) 81 (56) 82 (36)	68 (100) 99 (11)	68 (58) 115 (100)	68 (21) 81 (61) 149 (38) 159 (46) 160 (100)	68 (100) 99 (7)	68 (78) 81 (42) 115 (32) 116 (100) 159 (9)	68 (100) 149 (79)	68 (100) 117 (8)
pyrrole	67 (100)	67 (100) 80 (18)	67 (100) 80 (5)	67 (100) 80 (53) 81 (6)	67 (100) 98 (18)	67 (100) 114 (8)	67 (100) 80 (25) 158 (8) 159 (37)	67 (100) 114 (7)	67 (100) 80 (10) 114 (4) 115 (14)	67 (100) 148 (18)	67 (100) 116 (4)
pyridine	79 (97) 80 (100)	80 (100) 93 (8) 128 (87)	80 (100) 93 (48)	80 (85) 93 (100)	80 (100) 159 (18)	80 (100) 159 (31)	80 (100) 159 (17)	80 (100) 159 (9)	80 (100) 159 (6)	80 (1) 196 (100)	80 (100) 148 (5) 159 (4)

reactions may occur via the same ion/molecule addition product of molecular oxygen and the ionized carbene. These reactions occur for X = Y = Br, X = Br, and Y = Cl but not when X = Y = F and X = Y = Cl.

Morton et al.[8] examined the gas-phase metathesis reactions of $^+CF_3$ with carbonyl compounds using chemical ionization and tandem mass spectrometry combined with density functional theory (DFT) calculations. The proposed mechanism assumes the addition of $^+CF_3$ to the carbonyl oxygen followed by transposition via a four-membered cyclic transition state (eq 4).

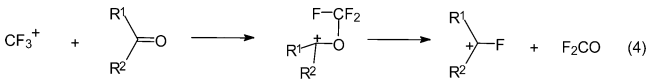

(4)

O'Hair and Gronert[9] studied the gas-phase reactions of the substituted methyl cations $^+CH_2X$ (X = F, HO, or Cl) with formamide. These carbocations were found to add to the nitrogen atom to form N-adducts, which are less stable than the corresponding O-adducts. Fragmentation of the N-adduct via a transition state involving a 1,3[HCO]$^+$ transfer to yield HC(O)X and $^+CH_2NH_2$ was only found for $^+CH_2OH$ and $^+CH_2Cl$. A novel CO extrusion reaction via N-adducts was also observed for $^+CH_2F$ and $^+CH_2Cl$.

We recently reported that ^+CF reacts promptly with N_2O by O abstraction to form the highly electrophilic acylium ion FCO^+, which was used to functionalize the relatively inert Ar−H bonds of benzene and some heterocycles via gas-phase carbonylation (eq 5).[10]

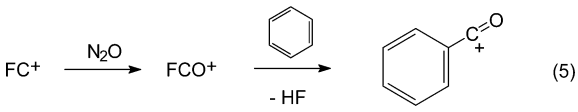

(5)

Herein, we report a systematic study of the gas-phase reactivity of several halocarbocations, $^+CH_2X$ (X = Cl, Br, or I), $^+CHX^1X^2$ (X = F, Cl, or Br), and $^+CX_3$ (X = F or Cl), with four prototype aromatic compounds: benzene, furan, pyrrole, and pyridine. The halocarbocations are strong Lewis acids because they contain an empty p orbital, and as a consequence, it is expected that they could react promptly with these rich π-electron aromatic compounds. Hence, the reactants were specifically chosen to verify the effect on reactivity as we change the nature of the aromatic ring as well as the type (C−X bond strength) and number of halogen substituents on the halocarbocations.

Experimental Section

The experiments were performed in an Extrel (Pittsburgh, PA) pentaquadrupole ($Q_1q_2Q_3q_4Q_5$) mass spectrometer.[11] The instrument is composed of a sequential arrangement of three mass analyzing (Q_1, Q_3, and Q_5) and two "rf-only" ion-focusing reaction quadrupoles (q_2 and q_4). Gaseous halocarbocations were generated in the ion source from the following neutral precursors by electron ionization (EI) using 70 eV electrons: CH_2Cl_2 ($^+CH_2Cl$), CH_2BrCl ($^+CH_2Br$), CH_3CH_2I ($^+CH_2I$), $CHClF_2$ ($^+CHF_2$), $CHCl_3$ ($^+CHCl_2$), $CHBr_2Cl$ ($^+CHBr_2$ and ^+CHBrCl), $CHClF_2$ (^+CHClF), CCl_4 ($^+CCl_3$), and CF_4 ($^+CF_3$). In the double-stage (MS^2) mass spectrometric experiments, Q_1 was used to mass-select the halocarbocations for further reactions in q_2 with a chosen aromatic compound. Ion translational energies were set to 1 eV as calibrated by the *m/z* 39:41 ratio in neutral ethylene/ionized ethylene reactions.[12] Product ion mass spectra were acquired by scanning Q_5, while operating Q_3 in the broad-band rf-only mode. Multiple collision conditions that caused typical beam attenuations of 50−70% were used in q_2 so as to increase the reaction yields and to promote the collisional quenching of both the reactant and product ions.[13] Reactant ions should therefore display no or negligible amounts of excess internal energy. For the MS^3 experiments, Q_3 was used to mass-select a q_2 product ion of interest for further 15 eV collision-induced dissociation with argon or 1 eV ion/molecule reactions with a neutral reactant in q_4, while scanning Q_5 to acquire the product ion mass spectrum. The 15 and 1 eV collision energies were taken as the voltage difference between the ion source and the collision quadrupoles. The indicated pressures in each differentially pumped region were typically 2×10^{-6} (ion source), 8×10^{-6} (q_2), and 8×10^{-5} Torr (q_4).

Results and Discussion

Table 1 summarizes the product ion mass spectra with the main products and relative abundances arising from the gas-phase reactions of the mass-selected $^+CH_nX_m$ halocarbocations with benzene, furan, pyrrole, and pyridine, all performed under low-energy conditions (~1 eV) and in the relatively high-pressure environment ($\sim 10^{-2}$ Torr) of quadrupole collision cells. The influence of the type, the bond strength, and the number of halogen substituents (π-type stabilization) on the intrinsic reactivity of these halocarbocations toward the four prototype aromatic compounds can be therefore evaluated and compared with that of the simplest $^+CH_3$ carbocation. Table 2 summarizes the sequential product ion mass spectra for CID of major mass-

TABLE 2: Main Fragment Ions Observed in the Triple-Stage (MS^3) Spectra for CID of Main Product Ions Arising from Reactions of the Halocarbocations with the Four Prototype Aromatic Compounds

aromatic compound	halocarbocation	product (*m*/*z*)	CID fragments *m*/*z* (% relative abundance)
benzene	CH_2Cl^+, CH_2Br^+, H_2I^+, $CHBr_2^+$	91	65 (100), 41 (3), 39 (9)
	CHF_2^+, $CHClF^+$	109	83 (100)
	$CHCl_2^+$, $CHBrCl^+$	125	99 (25), 90 (62), 89 (100)
	CF_3^+	127	101 (100)
	CCl_3^+	159	133 (8), 124 (86), 123 (100),99 (9), 89 (97)
	$CHBr_2^+$, $CHBrCl^+$	169	90 (100), 89 (32), 63 (2)
furan	CH_2Cl^+, CH_2Br^+, CH_2I^+, $CHBr_2^+$, $CHBrCl^+$	81	53 (100), 27 (7)
	CHF_2^+, $CHClF^+$	99	71 (100)
	CF_3^+	117	89 (100)
	CH_2I^+	82	81 (78), 54 (100)
	$CHCl_2^+$, $CHBrCl^+$	115	87 (36), 51 (100)
	$CHBrCl^+$	116	81 (100), 53 (6)
	CCl_3^+	149	121 (100), 85 (7)
	$CHBr_2^+$, $CHBrCl^+$	159	131 (37), 91 (100), 51 (13)
	$CHBr_2^+$	160	81 (100), 53 (2)
pyrrole	CH_2Cl^+, CH_2Br^+, CH_2I^+, $CHBr_2^+$, $CHBrCl^+$	80	53 (100)
	$CHBr_2^+$	158	131 (9), 79 (100)
	CHF_2^+, $CHClF^+$	98	71 (100)
	CF_3^+	116	89 (100)
	$CHBr_2^+$	159	80 (100)
pyridine	$CHBr_2^+$, CH_2I^+	93	92 (7), 78 (4), 67 (8), 66 (100), 65 (38)
	CCl_3^+	196	117 (100)

selected product ions, which are used for structural characterization.

$^+CH_3$. Under low-energy collisions (1 eV) of the quadrupole reaction cell, the mass-selected and relatively cold $^+CH_3$ cation (quenched by low-energy collisions with the neutral), with a recombination energy (RE) value of 9.84 eV[14] and a proton affinity (PA) value for the corresponding neutral carbene ($:CH_2$) of 866.1 kJ mol^{-1},[15] reacts with benzene (IE = 9.25 eV; PA = 750.2 kJ/mol), furan (IE = 8.88 eV; PA = 803.3 kJ mol^{-1}), pyrrole (IE = 8.21 eV; PA = 871.1 kJ mol^{-1}), and pyridine (IE = 9.26 eV; PA = 928.9 kJ mol^{-1}),[15] mainly by electron abstraction, yielding exclusively the respective ionized aromatic

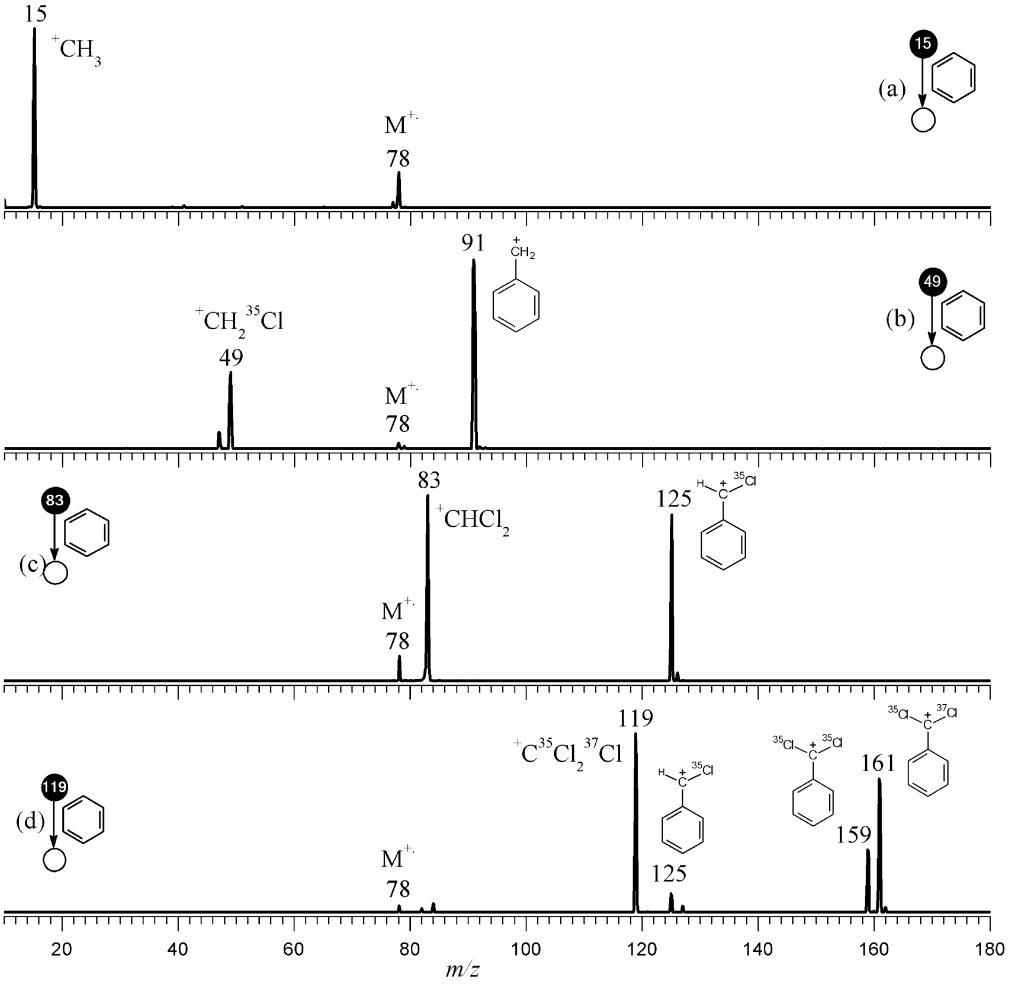

Figure 1. Double-stage (MS^2) product ion mass spectra for reactions of benzene with (a) $^+CH_3$, (b) $^+CH_2{}^{35}Cl$, (c) $^+CH^{35}Cl_2$, and (d) $^+C^{35}Cl_2{}^{37}Cl$.

molecules (ionized benzene of *m*/*z* 78 in Figure 1a). For only the basic pyridine are both the ionized (*m*/*z* 79) and protonated molecules (*m*/*z* 80) detected (Table 1).

Although $^+CH_3$ could be predicted to act as a potent electrophile, adding efficiently to electron-rich aromatic compounds, its relatively high recombination energy of 9.84 eV[15] favors, however, electron abstraction. $^+CH_3$ behaves therefore predominantly as a potent oxidant. Proton transfer from $^+CH_3$ is also energetically favored in reactions with basic aromatic compounds such as pyridine.

$^+CH_2X$ (X = Cl, Br, or I). *Benzene, Furan, and Pyrrole.* The monohalogenated carbocations $^+CH_2Cl$ (8.75 eV),[16] $^+CH_2Br$ (8.61 eV),[16] and $^+CH_2I$ (8.40 eV)[16] have recombination energies (RE) that are considerably less than that of $^+CH_3$ (9.84 eV);[16] hence, they still react with the four prototype aromatic compounds (Ar−H) by electron abstraction. However, for the $^+CH_2X$ cations, $[Ar-CH_2]^+$ functionalization via H−X loss from the nascent and unstable adduct occurs competitively. $[Ar-CH_2]^+$ functionalization is therefore favored over the $[Ar-CHX]^+$ functionalization that would otherwise require the loss of H_2. This trend can be rationalized by comparing the weakness of the C−X bonds (X = Cl, Br, or I) to the C−H bond (see discussion on bond energies below). With benzene (IE = 9.25 eV),[15] $[Ar-CH_2]^+$ functionalization (net ^+CH transfer) dominates for the reactions with the three $^+CH_2X$ ions and forms major product ions of *m*/*z* 91 (Scheme 1), as exemplified for

SCHEME 1

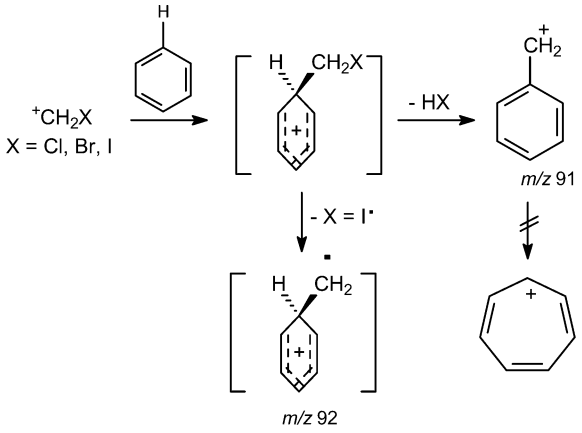

$^+CH_2Cl$ in Figure 1b. If the impetus to promote $[Ar-CH_2]^+$ functionalization is compared with that of abstracting an electron from benzene (relative yields of the respective products), the reactivity order is $^+CH_2Cl$ > $^+CH_2Br$ > $^+CH_2I$. This reactivity order corresponds to the inverse of the recombination energy order and correlates well with the relative bond order for the released H−X molecules, that is, H−Cl > H−Br > H−I.

Although the isomeric seven-membered ring aromatic tropylium ion is nearly −42 kJ mol^{-1} more stable than the benzylium ion,[17] the heat liberated in these exothermic reactions is calculated (see below) to be insufficient for inducing isomerization of the nascent benzylium ion. The relatively heavy leaving neutral H−X should also carry away a considerable amount of the internal energy of the nascent adduct.

In electrophilic substitutions, furan and pyrrole are much more reactive than benzene and resemble the most reactive benzene derivatives. However, the relatively low IEs of these molecules should also favor electron abstraction. In reactions with $^+CH_2X$, the $[Ar-CH_2]^+$ functionalization of furan (Figure 2a) and pyrrole still occurs to a considerable extent (Table 1), but the electron abstraction that forms the respective ionized molecules of *m*/*z* 68 and 67 becomes the major reaction. Like the reactions with benzene, the $[Ar-CH_2]^+$ functionalization of furan and pyrrole (Scheme 2) likely yields the relatively cold 2-furanyl-

SCHEME 2

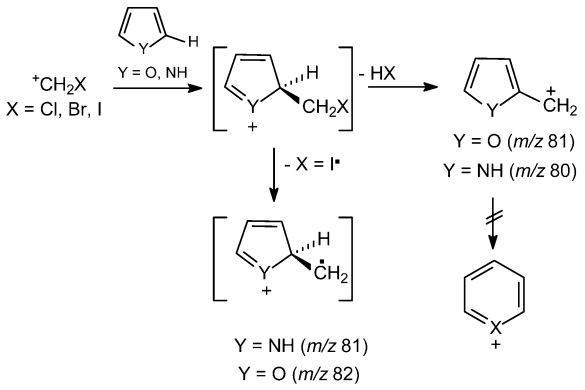

methyl (*m*/*z* 81) and 2-pyrrolylmethyl (*m*/*z* 80) cations[18] with an internal energy insufficient for overcoming the barriers for isomerization to the more-stable pyrilium and protonated pyridine cations, respectively. With furan and pyrrole, a different reactivity order (as compared with benzene) for the $[Ar-CH_2]^+$ functionalization versus electron abstraction is observed: $^+CH_2I$ > $^+CH_2Cl$ > $^+CH_2Br$.

Net $[CH_2]^{+\bullet}$ Transfer. Reactions of the iodomethyl cation, $^+CH_2I$, are interesting since an additional and unique channel is observed: net $[CH_2]^{+\bullet}$ transfer that forms the product ions of *m*/*z* 92 (benzene), 82 (furan), and 81 (pyrrole). Although such a product is minor for benzene and pyrrole, it is particularly abundant for furan (*m*/*z* 82, Figure 2a). The loss of the iodine atom from the nascent adduct (Schemes 1 and 2) likely leads to nascent, not easily accessible distonic ions.[19,20] These distonic ions are less stable than the two alternative conventional radical cation structures formed by a [1,2-H] shift or ring expansion (Scheme 3). For the toluene distonic ion, the barrier for the

SCHEME 3

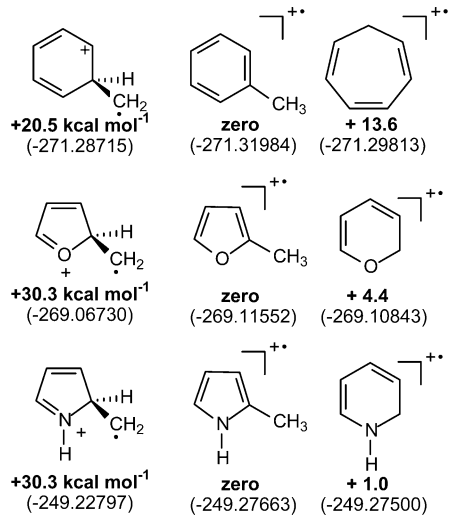

[1,2-H] shift isomerization to the most stable conventional form of ionized toluene has been found to be higher than that leading to the ionized cycloheptatriene, which occupies an intermediate energy position.[21] Hence, whether the nascent distonic ion remains as such or isomerizes to one of its either more kinetically or more thermodynamically favored isomers will

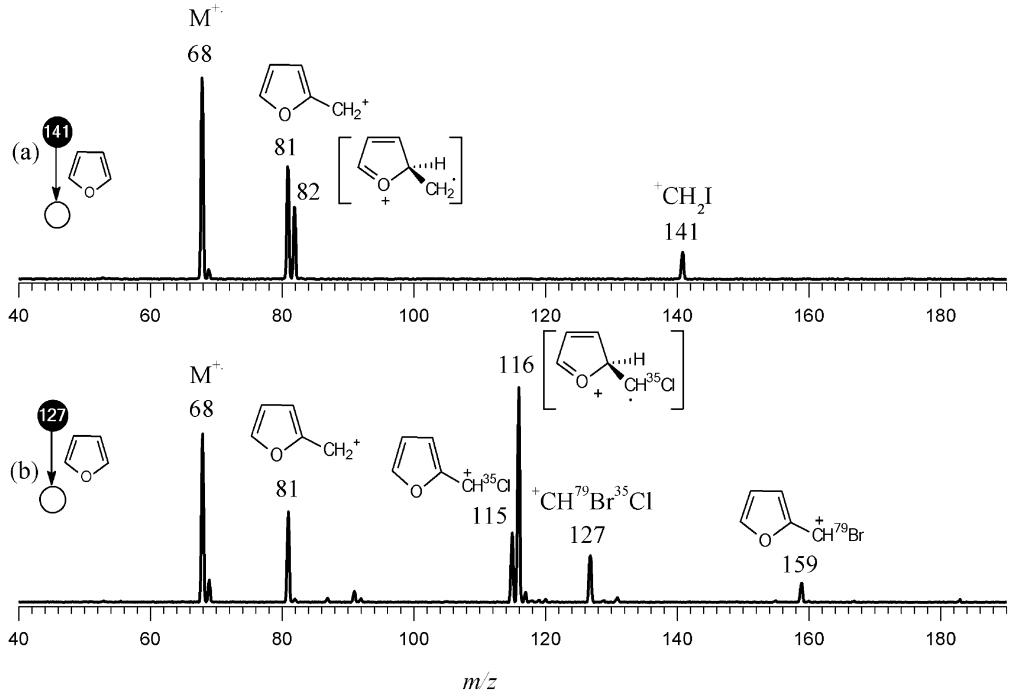

Figure 2. Double-stage (MS^2) product ion mass spectra for reactions of furan with (a) $^+CH_2I$ and (b) $^+CH^{79}Br^{35}Cl$.

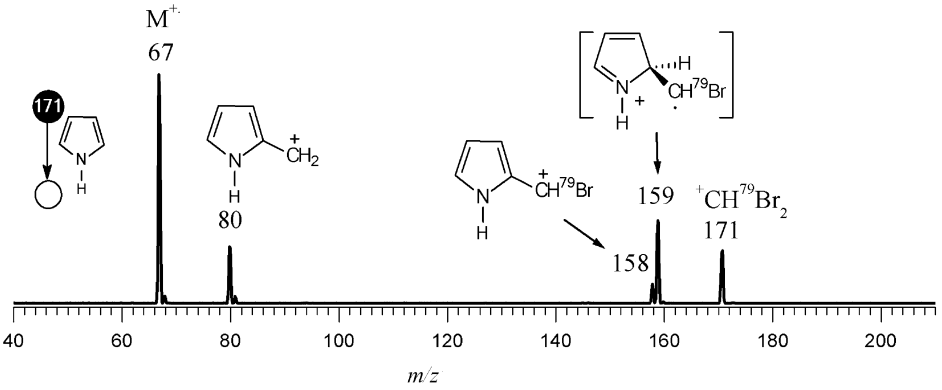

Figure 3. Double-stage (MS^2) product ion mass spectra for reactions of pyrrole with $^+CH^{79}Br_2$.

depend on its actual internal energy content, which is expected to be very low but difficult to measure. Similar energy profiles are likely to be displayed by the distonic forms of ionized 2-methylfuran, ionized 2-methylpyrrole (Scheme 2), and their conventional radical cation isomers.

Pyridine. With pyridine, no $[Ar-CH_2]^+$ functionalization products are detected, and the $^+CH_2X$ cations react extensively and distinctively by two major reactions: (i) proton transfer that forms protonated pyridine of *m*/*z* 80 and (ii) addition via the electrophilic attack to the nitrogen lone pair (Scheme 4),

SCHEME 4

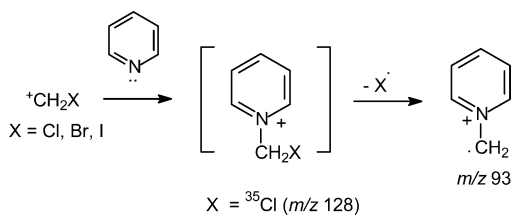

forming either stable or unstable adducts. The $^+CH_2Cl$/pyridine adduct of *m*/*z* 128 (Figure 4a) is quite stable and dissociates only scarcely by the loss of Cl• to form a product ion of *m*/*z* 93 (a net $CH_2^{+\bullet}$ transfer reaction). The pyridine adducts with $^+CH_2I$ (Figure 4b) and $^+CH_2Br$ (Table 1) are, however, considerably more prone to dissociation by halogen atom loss, thus, forming to great extents the same distonic *N*-methylene pyridinium ion of *m*/*z* 93.[22−25]

These experimental trends could be rationalized by considering the corresponding C−X bond energies: C−I (213) < C−Br (284) < C−Cl (339) < C−F (485 kJ mol^{-1}).[26] For instance, halogen atom loss from the nascent adducts of benzene, furan, and pyrrole (X = I, Br, or Cl; Schemes 1 and 2) is only observed for the $^+CH_2I$ adduct (I• loss) due to the relative weakness of the C−I bond. For the nascent adducts of benzene, furan, and pyrrole with $^+CHX^1X^2$ (X^1, X^2 = F, Cl, or Br; Schemes 5 and 6), only the bromine atom loss is detected, again, due to the relative weakness of the C−Br bond. Also, for the nascent adducts of benzene with $^+CX_3$ (X = F or Cl; Scheme 8), only Cl• loss is observed with no detection of the corresponding product from F• loss. Finally, for the $^+CH_2X$ adduct with pyridine, the Cl• loss is minor, whereas I• and Br• loss occurs to a great extent due to the decreasing strengths of the corresponding C−X bonds.

$^+CHX^1X^2$ (X^1, X^2 = F, Cl, or Br). *Benzene, Furan, and Pyrrole.* Generally, the halocarbocations $^+CHX^1X^2$ react with benzene, furan, and pyrrole by two competing pathways: (i) electron abstraction and (ii) $[Ar-CHX]^+$ functionalization

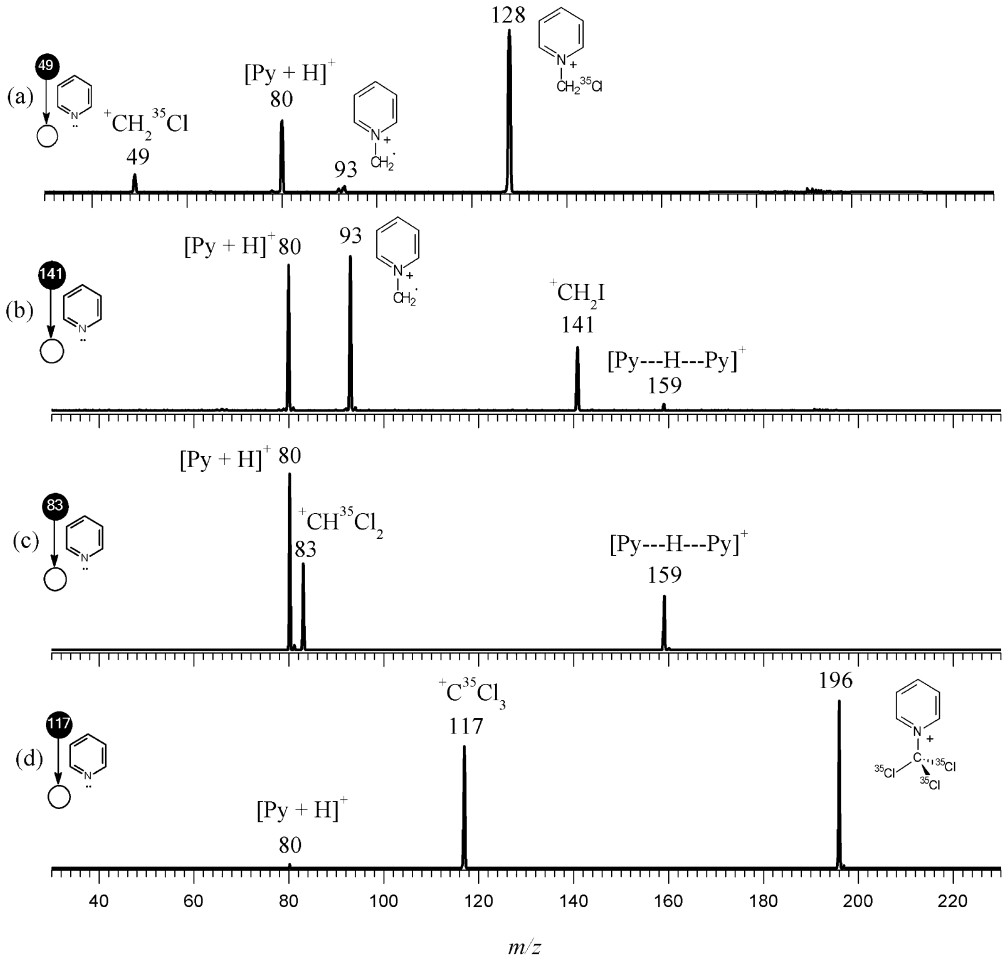

Figure 4. Double-stage (MS^2) product ion mass spectra for reactions of pyridine with (a) $^{+}CH_2{}^{35}Cl$, (b) $^{+}CH_2I$, (c) $^{+}CH^{35}Cl_2$, and (d) $^{+}C^{35}Cl_3$.

SCHEME 5

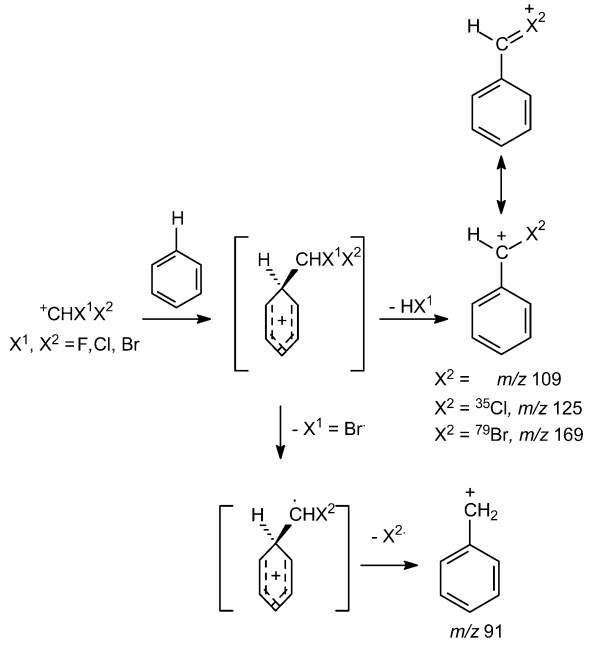

(Table 1). With benzene, the $[Ar-CHX]^{+}$ functionalization dominates and forms the respective α-fluorobenzylium ion of *m/z* 109, α-chlorobenzylium ion of *m/z* 125 (Figure 1c), and α-bromobenzylium ion of *m/z* 169 (Scheme 5). The dominance of the $[Ar-CHX]^{+}$ functionalization over electron abstraction

SCHEME 6

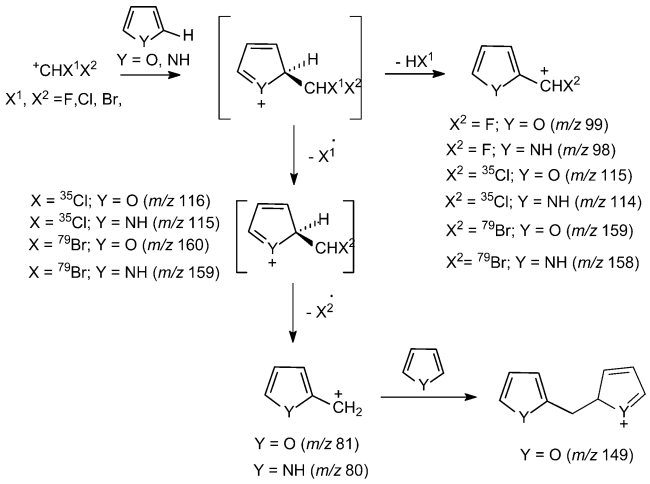

is facilitated from the carbocation stabilizing effect of the halogen atom, as shown by the halonium ion canonic form in Scheme 5. Like the reactions with $^{+}CH_2X$, electron abstraction becomes more favorable for furan and pyrrole (lower IEs than with benzene).[15] $[Ar-CHX]^{+}$ functionalization of furan and pyrrole (Figure 3) forms the α-halo 2-furanylmethyl and 2-pyrrolylmethyl cations, respectively (Scheme 6).

Only for the Br cations, $^{+}CHBr_2$ and $^{+}CHBrCl$, are additional reaction sequences often observed. Like the nascent adducts of $^{+}CH_2I$, which lose an iodine atom, the nascent $^{+}CHBr_2$ and

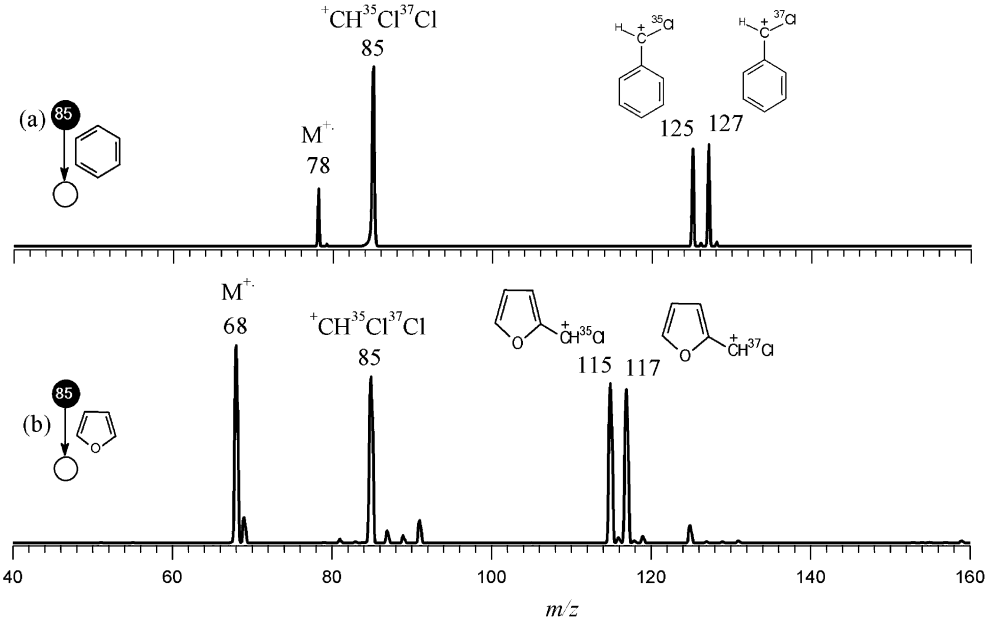

Figure 5. Double-stage (MS^2) product ion mass spectra for reactions of $^{+}CH^{35}Cl^{37}Cl$ with (a) benzene and (b) furan.

$^{+}$CHBrCl adducts also lose a bromine atom to form net $[CHBr]^{+\bullet}$ and $[CHCl]^{+\bullet}$ transfer products, respectively. With benzene, this product is not detected since it likely dissociates promptly by a second loss of either Br$^{\bullet}$ (Scheme 5) or Cl$^{\bullet}$ to form an ion of *m*/*z* 91 (Table 1). For furan, the net $[CHBr]^{+\bullet}$ and $[CHCl]^{+\bullet}$ transfer products, ionized 2-bromomethylfuran (*m*/*z* 160) and ionized 2-chloromethylfuran (*m*/*z* 116; Figure 2b), respectively, are detected as the most abundant product ions (Scheme 6), which dissociate by a second loss of either Br$^{\bullet}$ or Cl$^{\bullet}$ to form the 2-furanylmethyl cation of *m*/*z* 81. This product ion of *m*/*z* 81 associates further with furan to form an adduct of *m*/*z* 149 (Table 1), which is likely formed by a C2 electrophilic attack[18] as proposed in Scheme 6. For pyrrole (see, for instance, Figure 3), similar reaction sequences dominate, yielding product ions of *m*/*z* 159 and 115 from net transfers of $[CHBr]^{+\bullet}$ and $[CHCl]^{+\bullet}$, respectively. These ions dissociate to generate the 2-pyrrolylmethyl cation of *m*/*z* 80 (Table 1 and Scheme 6).

Pyridine. In the reactions of $^{+}CHX^1X^2$ (Figure 4c) with pyridine, again, no $[Ar-CHX]^{+}$ functionalization products are detected, and the proton transfer that yields protonated pyridine of *m*/*z* 80, and subsequently the pyridine proton-bound dimer of *m*/*z* 159, dominates (Table 1). Although proton transfer to pyridine could occur either directly from the reactant ions (Scheme 7, pathway a) or as a secondary reaction with the

SCHEME 7

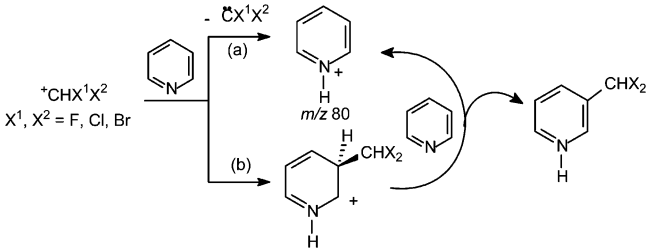

nascent adduct (pathway b), reactions with pyridine-d_5 yield only the protonated pyridine of *m*/*z* 80 (spectrum not shown). Therefore, proton transfer occurs directly from the reactant $^{+}CHX^1X^2$ cations. The preference for these halocarbocations to transfer a proton to basic pyridine arises, at least in part, from the great stability[27] of the dihalogenated carbene neutral products $:CX^1X^2$ and, consequently, from their relatively low proton affinity (for instance, 860.2 kJ mol^{-1} for $:CCl_2$ versus 873.2 kJ mol^{-1} for :CHCl).[28]

Kinetic Isotope Effect. The dilute gas-phase environment of mass spectrometers, in which a great variety of long-lived gaseous ions can be formed and isolated, has been used to conveniently measure many intrinsic kinetic isotope effects.[29−35] The isotope-mixed gaseous ions $^{+}CH^{35}Cl^{37}Cl$ and $^{+}CH^{79}Br^{81}Br$ give us the opportunity to measure the kinetic effect of $[Ar-CHX]^{+}$ functionalization. In reactions of $^{+}CH^{35}Cl^{37}Cl$ (Figure 5a), the $[Ar-CH^{37}Cl]^{+}$ functionalization of benzene (*m*/*z* 127) is found to be slightly more favored than the $[Ar-CH^{35}Cl]^{+}$ functionalization (*m*/*z* 125). Hence, the $H^{35}Cl$ loss from the intact adduct is slightly faster than the $H^{37}Cl$ loss, which characterizes a *normal* kinetic isotope effect (K_i = 1.025). $[Ar-CHBr]^{+}$ functionalization of benzene by $^{+}CH^{79}Br^{81}Br$ also shows a normal isotopic effect as the product ion $[Ar-CH^{81}Br]^{+}$ of *m*/*z* 171 ($H^{79}Br$ loss) is slightly favored over $[Ar-CH^{79}Br]^{+}$ of *m*/*z* 169 ($H^{81}Br$ loss) (K_i = 1.033) (data not shown). However, in reactions of $^{+}CH^{35}Cl^{37}Cl^{+}$ with furan (Figure 5b), the lighter $[Ar-CH^{35}Cl]^{+}$ product ion of *m*/*z* 115 ($H^{37}Cl$ loss) is slightly more favored than $[Ar-CH^{37}Cl]^{+}$ of *m*/*z* 117, which characterizes an inverse kinetic isotope effect (K_i = 0.970).

$[Ar-CHX^1]^{+}$ versus $[Ar-CHX^2]^{+}$ Functionalization. The "halogen-mixed" cations $^{+}$CHClF and $^{+}$CHClBr provide us the unique opportunity to evaluate the competition between the $[Ar-CHCl]^{+}$ versus $[Ar-CHF]^{+}$ and the $[Ar-CHCl]^{+}$ versus $[Ar-CHBr]^{+}$ functionalizations (Table 1). In reactions of $^{+}$CHClF with benzene (Figure 6b), $[Ar-CHF]^{+}$ of *m*/*z* 109 is formed exclusively (HCl loss) with no detectable $[Ar-CHCl]^{+}$ from HF loss (*m*/*z* 125). In reactions of $^{+}$CHClF with furan, $[Ar-CHF]^{+}$ of *m*/*z* 99 (HCl loss) is also formed exclusively (Table 1) with no detectable $[Ar-CHCl]^{+}$ of *m*/*z* 115 (HF loss). Note the preference for the loss of the heavier H−X neutral molecule and for the formation of the lighter α-halobenzylium ion.

To generate H−Cl and $[Ar-CHF]^{+}$ from the dissociation of the nascent $[Ar-CHClF]^{+}$ adduct, the C−H (414 kJ mol^{-1}) and C−Cl (339 kJ mol^{-1}) bonds are broken, and the H−Cl (431 kJ/mol) and C═C (610 kJ mol^{-1}) bonds are formed (Scheme 5).[26]

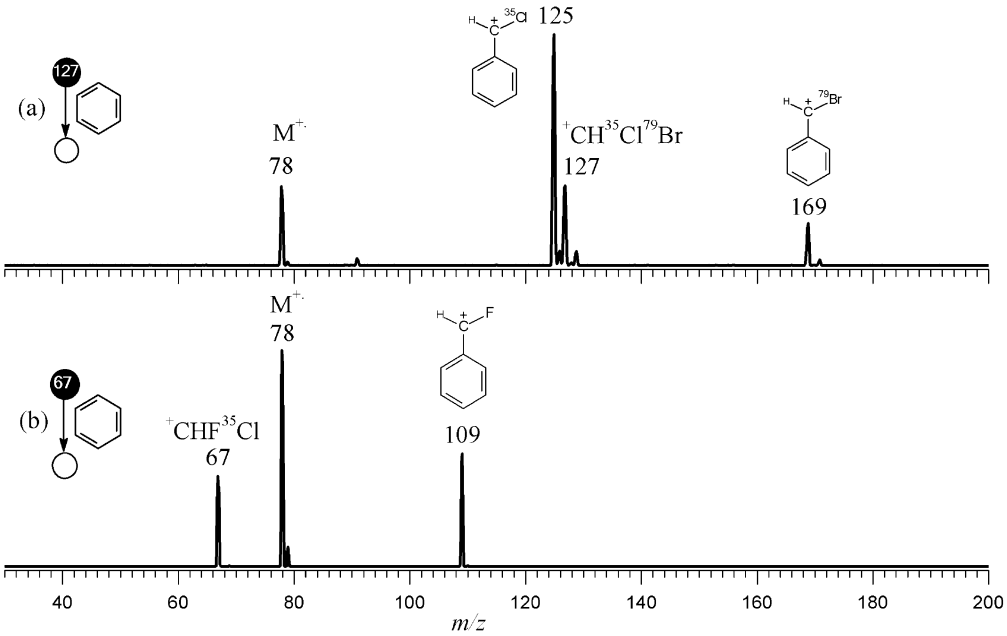

Figure 6. Double-stage (MS^2) product ion mass spectra for reactions of benzene with (a) $^+CH^{35}Cl^{79}Br$ and (b) $^+CHF^{35}Cl$.

Hence, the reaction enthalpy (ΔH), roughly estimated as $\sum(BE_{broken}) - \sum(BE_{formed})$, is -288 kJ mol^{-1}. To generate H−F and [Ar−CHCl]$^+$, however, the C−H (414 kJ mol^{-1}) and C−F (485 kJ mol^{-1}) bonds are broken, whereas the H−F (568 kJ mol^{-1}) and C═C (610 kJ mol^{-1}) bonds are formed,[26] leading to a less exothermic process (-279 kJ mol^{-1}). Thus, these roughly estimated energetic data are, in this case, consistent with the experimental results, which show the predominance of H−Cl loss over H−F loss.

The nascent [Ar−CHClBr]$^+$ adducts, formed from the reaction between benzene or furan with $^+$CHClBr, dissociate predominantly again by the loss of the heavier H−X molecule, that is, by H−Br loss rather than H−Cl loss. For instance, with benzene (Figure 6a), [Ar−CHCl]$^+$ of *m*/*z* 125 is greatly favored over [Ar−CHBr]$^+$ of *m*/*z* 169, and with furan (Figure 2b), [Ar−CHCl]$^+$ of *m*/*z* 115 is also greatly favored over [Ar−CHBr]$^+$ of *m*/*z* 159. For the H−Cl loss dissociation pathway [broken bonds: C−H (414 kJ mol^{-1}) and C−Cl (339 kJ mol^{-1}); bonds formed: H−Cl (431 kJ mol^{-1}) and C═C (610 kJ mol^{-1})],[26] a reaction enthalpy of -288 kJ mol^{-1} is calculated. However, for the predominant dissociation process by the H−Br loss, for which the C−H (414 kJ mol^{-1}) and C−Br (284 kJ mol^{-1}) bonds are broken and the H−Br (365 kJ mol^{-1}) and C═C (610 kJ mol^{-1}) bonds are formed,[26] a less exothermic process (-277 kJ mol^{-1}) is obtained. This discrepancy (the less exothermic process as calculated by bond energies dominates) likely results from the substantial differences in product stability and entropic factors that are associated with both competitive processes. With the heavier molecule, correlating to a weaker H−X bond [H−F (568), H−Cl (431), and H−Br (365 kJ mol^{-1})], the preference for the loss of the heavier molecule indicates that the formation of the more stable α-halobenzylium ion is the main factor governing preferential [Ar−CHX]$^+$ functionalization. Therefore, more stable α-fluorobenzylium ion and α-fluoro-2-furanylmethyl cations are formed preferentially to the less stable α-chloro analogues, which are in turn formed preferentially to the less stable α-bromo analogues (see structures below). This order is consistent with the conventional wisdom that fluorine is a better electron donor than chloride regardless of its greater electronegativity because of the superior overlap between the fluorine and carbon 2p orbitals, and so on for the other halogens in the group.[36]

$^+CX_3$ (X = F or Cl). *$^+CF_3$.* Due to the presence of the three highly electrophilic fluorine atoms, $^+CF_3$ would be expected to be a very potent electrophile adding promptly to aromatic compounds.[37] $^+CF_3$ has, however, a recombination energy as high as 9.17 eV,[38] and should, therefore, also function as a potent oxidant and easily abstract an electron from "electron-rich" molecules. In reactions with benzene (Table 1), $^+CF_3$ reacts mainly by electron abstraction (*m*/*z* 78), and a minor [Ar−CF_2]$^+$ product of *m*/*z* 127 is formed concurrently (Scheme 8). $^+CF_3$ also reacts to some extent with furan and pyrrole (Scheme 9) to form [Ar−CF_2]$^+$ ions of *m*/*z* 117 and 116, respectively, but again, for these more easily ionized heterocycles, electron abstraction dominates (Table 1). With pyridine, surprisingly (since $^+CF_3$ has no proton), protonated pyridine of *m*/*z* 80 and the pyridine proton dimer of *m*/*z* 159 are formed nearly exclusively, whereas the [pyridine−CF_3]$^+$ adduct of *m*/*z* 148 is observed as a minor product (Table 1). A possible source of protons requires that $^+CF_3$ add to pyridine and then a second pyridine molecule promptly abstract a proton from the nascent and acidic adduct via a mechanism similar to that depicted in Scheme 7b. Although this is a secondary reaction that would therefore be disfavored at low pressures (with greater relative yields of the adduct), insignificant changes in product ion distribution were observed with a great variation of pyridine pressure in the reaction chamber.

$^+CCl_3$. The trichloromethyl cation, with a relatively low recombination energy of 8.06 eV,[39] promptly reacts with benzene (IE = 9.25 eV)[15] (Figure 1d for the isotopically mixed $^+C^{35}Cl_2{}^{37}Cl$ cation) by [Ar−CCl_2]$^+$ functionalization to yield (nearly exclusively) isotopologue α,α-dichlorobenzoyl cations (of *m*/*z* 159 and 161 for $^+C^{35}Cl_2{}^{37}Cl$; Scheme 8). Carbocation cross-resonance with the two chlorine atoms should greatly stabilize the [Ar−CCl_2]$^+$ products of $^+CCl_3$. A minor product of *m*/*z* 125 is also observed, which is likely the [Ar−$CH^{35}Cl$]$^+$ ion formed via double-Cl$^\bullet$ loss from the nascent and unstable adduct (Scheme 8).

The $^+CCl_3$ halocarbocation reacts similarly with furan and pyrrole to yield the [Ar−CCl_2]$^+$ ions of *m*/*z* 149 and 148,

SCHEME 8

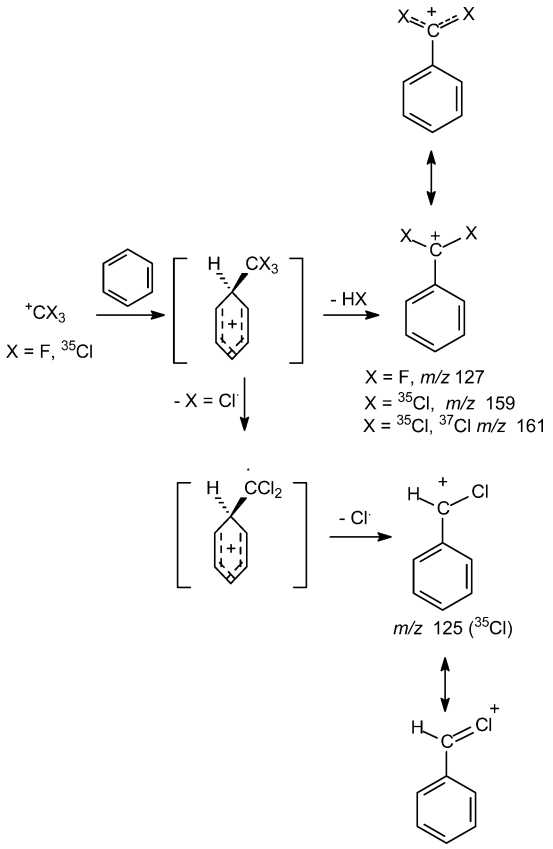

respectively (Scheme 9). Again, for these more easily ionized heterocycles, electron abstraction dominates (Table 1).

SCHEME 9

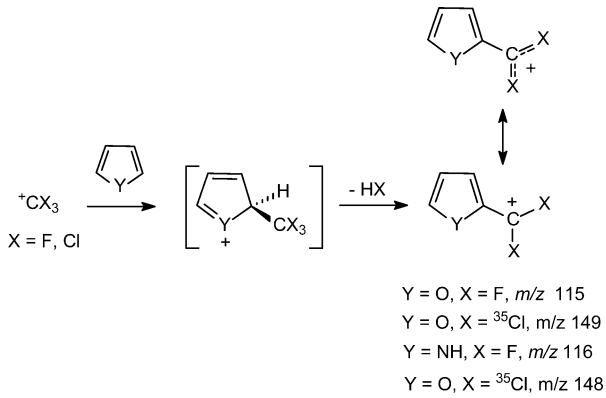

$^{+}CCl_3$, an ion with a relatively low recombination energy (8.06 eV)[39] and no acidic proton, reacts distinctively with pyridine (Figure 4d) compared to all other halocarbocations herein investigated. It forms promptly, and nearly exclusively (Table 1), an abundant and stable adduct of *m*/*z* 196 (Scheme 10) that shows no tendency to dissociate under the low-energy collisions employed in the quadrupole reaction cell. Formation of stable N-adducts with even electron cations is common for pyridine.[40,41]

SCHEME 10

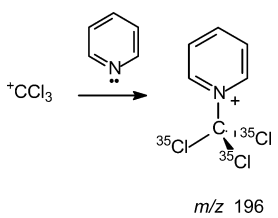

MS^3 Spectra. *Benzylium Ions.* All of the putative benzylium ions that were formed from the $[Ar-CH_2]^+$ or $[Ar-CHX]^+$ functionalization of benzene (Schemes 1 and 5) show considerable resistance toward collision-induced dissociation, which is likely due to their resonance-stabilized structures. The benzylium ion of *m*/*z* 91, the α-fluorobenzylium ion of *m*/*z* 109 (Figure 7a), and the α,α-difluorobenzylium ion of *m*/*z* 127 dissociate mainly by acetylene loss to form the fragment ions of *m*/*z* 65, 83, and 101, respectively. However, the α-chlorobenzylium ion of *m*/*z* 125 (fragment ions of *m*/*z* 90 and 89), the α,α-dichlorobenzylium ion of *m*/*z* 159 (fragment ions of *m*/*z* 124 and 123, as well as that of *m*/*z* 89 via $^{35}Cl^{\bullet}$ loss from the ion of *m*/*z* 124), and the α-bromobenzylium ion of *m*/*z* 169 (fragment ions of *m*/*z* 90 and 89, Figure 7b) dissociate mainly by both $X^{\bullet}$ and H−X loss (Table 2).

2-Furanylmethyl Cations. CID of the putative 2-furanylmethyl cation of *m*/*z* 81, the 2-furanylfluoromethyl cation of *m*/*z* 99, and the 2-furanyldifluoromethyl cation of *m*/*z* 117 formed via the $[Ar-CH_2]^+$, $[Ar-CHF]^+$, and $[Ar-CF_2]^+$ functionalization of furan, respectively, dissociates mainly by the loss of CO to form the fragment ions of *m*/*z* 53, 71, and 89, respectively (Table 2). This CO loss also occurs promptly but is followed by the H−Cl and H−Br loss for the 2-furanylchloromethyl cation of *m*/*z* 115 (*m*/*z* 87 and 51, respectively; Figure 7c), the 2-furanylbromomethyl cation of *m*/*z* 159 (*m*/*z* 131 and 51, respectively), and the 2-furanyldichloromethyl cation of *m*/*z* 149 (*m*/*z* 121 and 85, respectively).

2-Pyrrolylmethyl Cations. The putative 2-pyrrolylmethyl cation of *m*/*z* 80, the 2-pyrrolylfluoromethyl cation of *m*/*z* 98, and the 2-pyrrolyldifluoromethyl cation of *m*/*z* 116 formed via the $[Ar-CH_2]^+$, $[Ar-CHF]^+$, and $[Ar-CF_2]^+$ functionalization of pyrrole, respectively, dissociates mainly by the loss of HCN to form the fragment ions of *m*/*z* 53, 71, and 89, respectively (Table 2). The 2-pyrrolylbromomethyl cation of *m*/*z* 158 (Figure 7d) also loses HCN (*m*/*z* 131), but its main dissociation occurs by $Br^{\bullet}$ loss (*m*/*z* 79).

The N-Methylene and the α,α,α*-Trichloromethylpyridinium Ions.* The distonic radical cation of *m*/*z* 93 (Figure 8a), formed by the net CH_2^+ transfer to pyridine, likely dissociates by the loss of $H^{\bullet}$ (*m*/*z* 92), a methyl radical (*m*/*z* 78), acetylene (*m*/*z* 67), HCN (*m*/*z* 66), and $H^{\bullet}$ plus HCN (*m*/*z* 65). This dissociation chemistry is the same as that of the authentic *N*-methylene pyridinium ion that was formed via ionized methylene transfer from the α-distonic ion $^{+}CH_2-O-CH_2^{\bullet}$ to pyridine.[24] The α,α,α-trichloromethylpyridinium ion of *m*/*z* 196 dissociates solely by the loss of neutral pyridine to re-form $C^{35}Cl_3^+$ of *m*/*z* 117 (Table 2).

The Nascent Distonic Forms of Ionized 2-Methylfuran, α*-Chloromethylpyrrole,* α*-Bromomethylfuran, and* α*-Bromomethylpyrrole.* The relatively abundant net $CH_2^{+\bullet}$ transfer product to furan of *m*/*z* 82 (Figure 8b), that is, the nascent distonic form of ionized 2-methylfuran, dissociates mainly by both $H^{\bullet}$ loss (*m*/*z* 81) and CO loss (*m*/*z* 54). This is the same dissociation chemistry displayed by the conventional form of ionized 2-methylfuran, but it should not be taken as evidence that such an ion has been sampled since, like ionized toluene and its isomers,[22] barriers for isomerization may lay below the dissociation thresholds. The nascent distonic form of ionized α-chloromethylpyrrole of *m*/*z* 116 (Table 2) dissociates by the loss of both $Cl^{\bullet}$ (*m*/*z* 81) and CO (*m*/*z* 53). The nascent distonic forms of ionized α-bromomethylfuran of *m*/*z* 160 (Figure 7c)

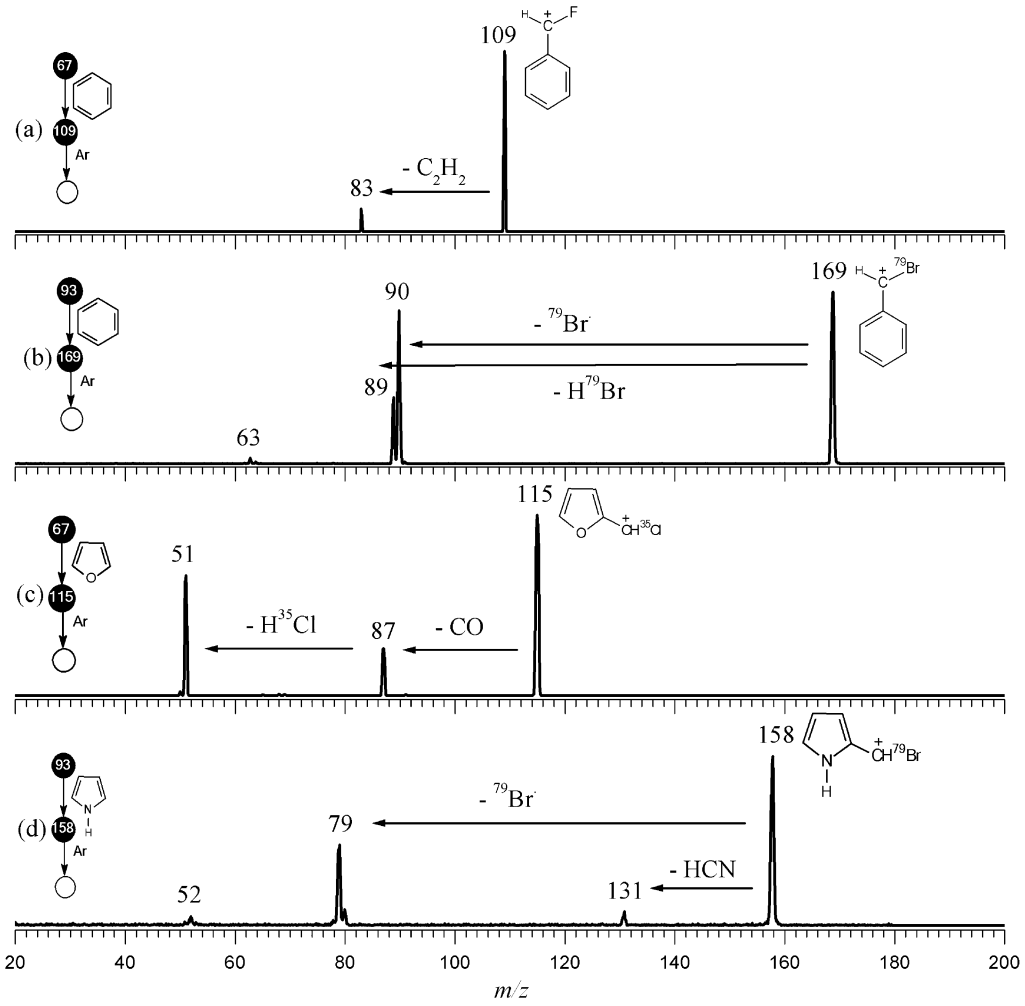

Figure 7. Triple-stage (MS^3) CID product ion mass spectra for the (a) α-fluorobenzylium ion of *m*/*z* 109, (b) α-bromobenzylium ion of *m*/*z* 169, (c) 2-furanylchloromethyl cation of *m*/*z* 115, and (d) 2-pyrrolylbromomethyl cation of *m*/*z* 158.

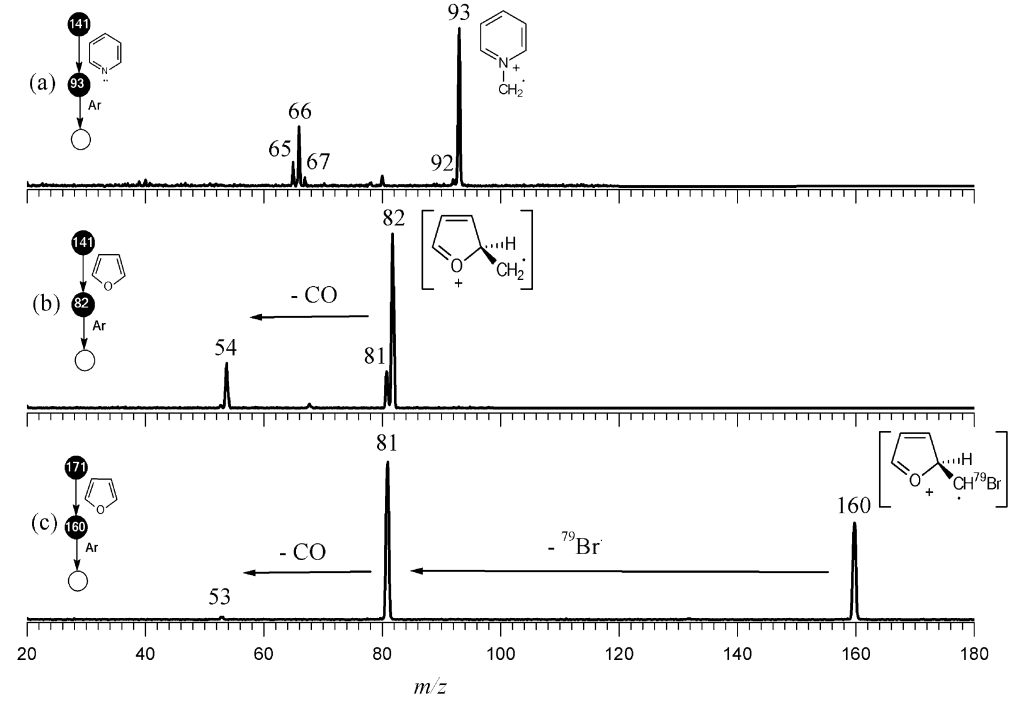

Figure 8. Triple-stage (MS^3) CID product ion mass spectra for the (a) distonic radical cation of *m*/*z* 93 formed by the net-ionized methylene transfer to pyridine, (b) ionized 2-methylfuran of *m*/*z* 82, and (c) ionized α-bromomethylfuran of *m*/*z* 160.

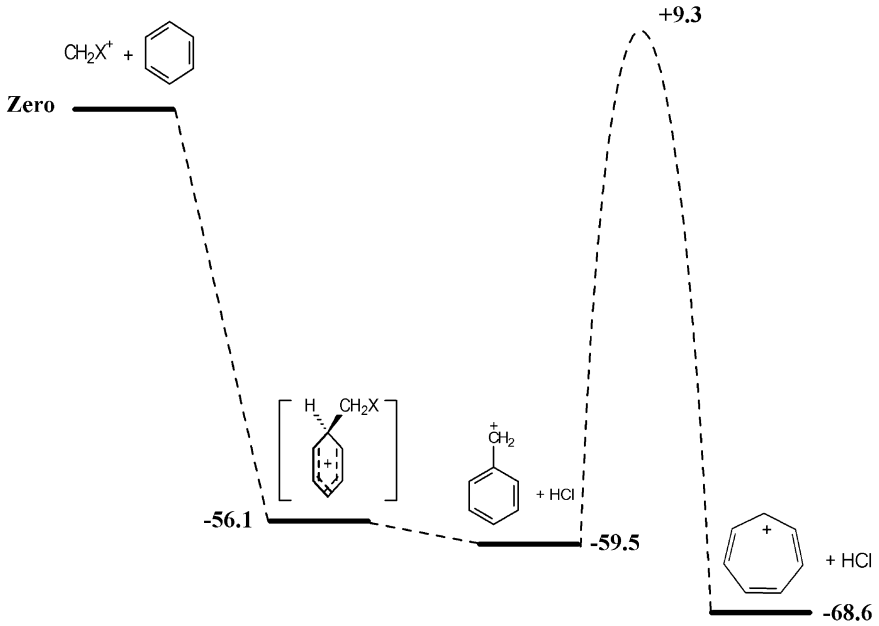

Figure 9. B3LYP/6-31G(d,p) energy changes for the reaction between benzene and the halocarbocation $^{+}CH_2Cl$. Energies are given in kilocalories per mole (1 kcal = 4.18 kJ).

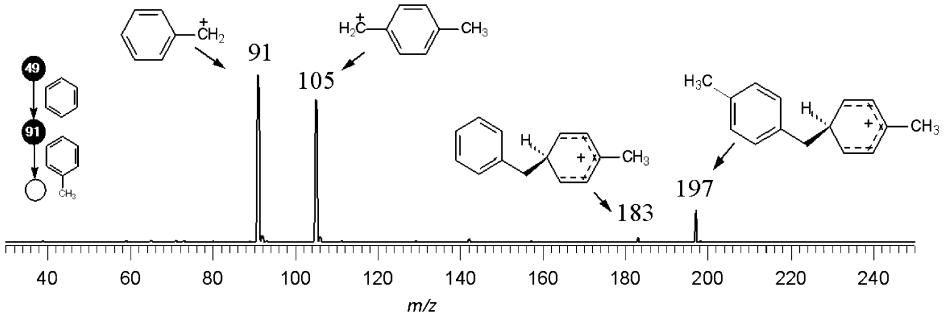

Figure 10. Triple-stage (MS^3) product ion mass spectra for the reaction between benzylium ion of *m*/*z* 91 and toluene.

and α-bromomethylpyrrole of *m*/*z* 159 (Table 2) dissociate promptly by the loss of Br• to form the fragment ions of *m*/*z* 81 and 80, respectively, and then scarcely by the CO loss.

Benzylium or Tropylium Ions? *Theoretical Calculations.* The isomerization of the benzylium ion to the more stable, fully aromatic tropylium ion has been extensively studied both experimentally and theoretically[42−46] in the long series of studies on this classic and fundamental dichotomy in gas-phase ion chemistry.[21] A recent theoretical calculation at the B3LYP/6-31G(d,p) level has estimated this isomerization barrier to lie 287.9 kJ mol^{-1} above the benzylium ion, and the tropylium ion to lie −38.1 kJ mol^{-1} below the benzylium ion.[17] To evaluate whether the nascent benzylium ions formed in the halocarbocation reactions herein described have enough energy to overcome such a barrier or if it would otherwise keep its "nascent" structure, the energetics for the reaction of $^{+}CH_2Cl$ with benzene were evaluated by B3LYP/6-31G(d,p) calculations (Figure 9). The results show that the nascent benzylium ion would have, at most, 249.0 kJ mol^{-1} of internal energy, which is 38.9 kJ mol^{-1} less than that required to overcome the barrier for isomerization to the tropylium ion. Additionally, the neutral H−X species (HCl in the case considered) certainly removes a considerable amount of such energy. Barriers for the isomerization of the furanylmethyl cation to the pyrilium ion and the pyrrolylmethyl cation to protonated pyridine have not been established, but it is reasonable to assume that these nascent ions are also not hot enough to undergo the ring expansion isomerization.[24]

Methylene Transfer Reactions with Toluene and Benzene. Ausloos[47] reacted $^{+}CD_2F$ with benzene to form $[C_7H_5D_2]^{+}$ ions and found that 90% of such ions react further with toluene to form $[C_8H_7D_2]^{+}$ via a structure-selective methylene transfer gas-phase ion/molecule reaction that characterizes the benzylium ion, whereas the tropylium ion was found to be unreactive. We have therefore performed, via MS^3 experiments, reactions of the putative benzylium ion formed in the functionalization reactions herein described with toluene. For instance, the $C_7H_7^{+}$ ion of *m*/*z* 91 formed in reactions of $^{+}CH_2{}^{35}Cl$ (*m*/*z* 49) with benzene reacts promptly with toluene (Figure 10) by the methylene transfer reaction to form the intact adduct of *m*/*z* 183 and mostly the *p*-xylenium ion of *m*/*z* 105 (Scheme 11). In the quadrupole collision cell, the ion of *m*/*z* 105 reacts further with toluene to form an intact adduct of *m*/*z* 197, which dissociates likewise to *m*/*z* 105.

The putative 2-furanylmethylium ion of *m*/*z* 81, formed in the reaction of $^{+}CH_2Cl$ with furan, was also observed to efficiently transfer methylene to toluene to form the 4-methylbenzylium ion of *m*/*z* 105 (Scheme 12). The putative 2-pyrrolylmethyl cation of *m*/*z* 80, formed in reactions of $^{+}CH_2Cl$ with pyrrole, was found, however, to be nearly unreactive toward toluene; hence, no firm conclusion about its primary structure can be drawn from this experiment.

The classic structure-selective methylene transfer reaction developed by Ausloos[47] for benzylium ions can be viewed to occur, in fact, by the exchange of methylene ($:CH_2$) by hydride

SCHEME 11

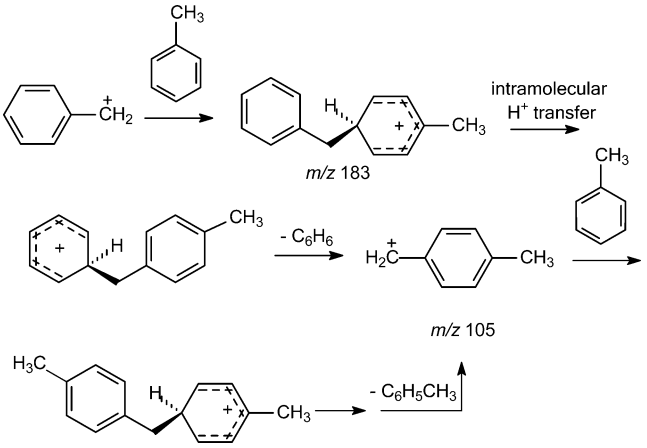

SCHEME 12

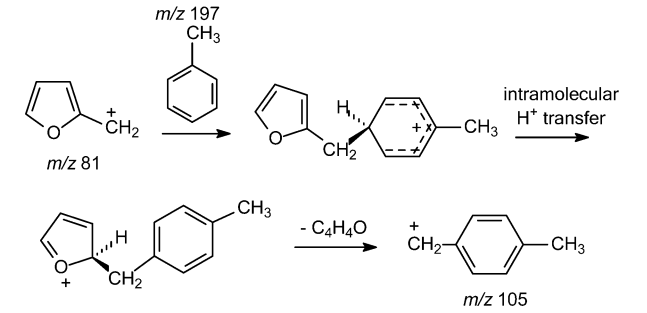

(:H$^-$). Schemes 11 and 12 offer more elaborate mechanisms for such reactions that expand the mechanism proposed by Ausloos.[47]

Conclusions

A systematic study of gas-phase reactivity of a set of halocarbocations, $^+CH_2X$ (X = Cl, Br, or I), $^+CHX^1X^2$ (X^1, X^2 = F, Cl, or Br), and $^+CX_3$ (X = F or Cl), with four prototype aromatic compounds, benzene, furan, pyrrole, and pyridine, was performed. With benzene, furan, and pyrrole, the $[Ar-CH_2]^+$, $[Ar-CHX]^+$, or $[Ar-X_2]^+$ functionalization with the activation of the relatively inert Ar−H bonds was observed as the major reaction, forming benzylium ions, 2-furanylmethyl, or 2-pyrrolylmethyl cations, respectively. Formation of nascent distonic ions, $[Ar-CH_2]^{+\bullet}$ or $[Ar-CHX]^{+\bullet}$, was also observed from the dissociation of nascent $[Ar-CH_2X]^+$ or $[Ar-CHX_2]^+$ adducts by the loss of a halogen atom, a process that is favored particularly for the heavier halogens (weaker C−X bonds). Kinetic isotope effects for the $[Ar-CHX]^+$ functionalization using naturally occurring halogen isotopes ($^{35}Cl/^{37}Cl$ and $^{79}Br/^{81}Br$) have been measured. Intrinsic competition for either the $[Ar-CHX^1]^+$ or $[Ar-CHX^2]^+$ functionalization using halogen-mixed halocarbocations $[CHX^1X^2]^+$ was evaluated. Formation of the lighter (more stable) α-halobenzylium ion associated with the loss of the heavier H−X molecule dominates. Similar functionalization reactions were not observed for pyridine; with this basic aromatic compound, the halocarbocations react by either proton transfer, N-addition, or net $CH_2^{+\bullet}$ transfer.

Acknowledgment. We thank the Research Support Foundation of the State of São Paulo (FAPESP) and the Brazilian National Research Council (CNPq) for financial support.

References and Notes

(1) Norris, J. F. *Am. Chem. J.* **1901**, *25*, 117.
(2) Kehrmann, F.; Wentzel, F. *Chem. Ber.* **1901**, *34*, 3815.
(3) Olah, G. A. *J. Org. Chem.* **2001**, *66*, 5943.
(4) O'Hair, R.-A. J. *Annu. Rep. Prog. Chem., Sect. B: Org. Chem.* **2001**, *97*, 393.
(5) Cacace, F.; de Petris, G.; Pepi, F.; Rosi, M.; Troiani, A. *Chem.—Eur. J.* **2000**, *6*, 2572.
(6) Mosi, A. A.; Cullen, W. R.; Eigendorf, G. K. *J. Mass Spectrom.* **1997**, *32*, 864.
(7) Pradeep, T.; Ma, S. G.; Shen, J. W.; Francisco, J. S.; Cooks, R. G. *J. Phys. Chem. A* **2000**, *104*, 6804.
(8) Nguyen, V.; Mayer, P. S.; Morton, T. H. *J. Org. Chem.* **2000**, *65*, 8032.
(9) O'Hair, R.-A. J.; Gronert, S. *Int. J. Mass Spectrom.* **2000**, *195—196*, 303.
(10) da Rocha, L. L.; Sparrapan, R.; Eberlin, M. N. *Int. J. Mass Spectrom.* **2003**, *228*, 901.
(11) Juliano, V. F.; Gozzo, F. C.; Eberlin, M. N.; Kascheres, C.; do Lago, C. L. *Anal. Chem.* **1996**, *68*, 1328.
(12) Tiernan, T. O.; Futrell, J. H. *J. Phys. Chem.* **1968**, *72*, 3080.
(13) Eberlin, M. N. *Mass Spectrom. Rev.* **1997**, *16*, 113.
(14) Lias, S. G.; Bartmess, J. E.; Liebman, J. F.; Holmes, J. L.; Levin, R. D.; Mallard, W. G. Ion Energetics Data. In *The NIST Chemistry WebBook*; Linstrom, P. J., Mallard, W. G., Eds.; National Institute of Standards and Technology: Gaithersburg, MD, 2001.
(15) Pliego, J. R.; DeAlmeida, W. B. *J. Chem. Soc., Faraday Trans.* **1997**, *93*, 1881.
(16) Andrews, L.; Dyke, J. M.; Jonathan, N.; Keddar, N.; Morris, A. *J. Am. Chem. Soc.* **1984**, *106*, 299.
(17) Ignatyev, I. S.; Sundius, T. *Chem. Phys. Lett.* **2000**, *326*, 101.
(18) Speranza, M. *Pure Appl. Chem.* **1991**, *63*, 243.
(19) Kenttamaa, H. I. *Org. Mass Spectrom.* **1994**, *29*, 1.
(20) Stirk, K. M.; Kiminkinen, L.-K. M.; Kenttamaa, H. I. *Chem. Rev.* **1992**, *92*, 1649.
(21) Lifshitz, C. *Acc. Chem. Res.* **1994**, *27*, 138.
(22) deKoster, C. G.; vanHoute, J. J.; vanThuijl, J. *Int. J. Mass Spectrom. Ion Processes* **1990**, *98*, 235.
(23) Gozzo, F. C.; Eberlin, M. N. *J. Am. Soc. Mass Spectrom.* **1995**, *6*, 554.
(24) Yu, S. J.; Holliman, C. L.; Rempel, D. L.; Gross, M. L. *J. Am. Chem. Soc.* **1993**, *115*, 9676.
(25) Yu, S. J.; Gross, M. L.; Fountain, K. R. *J. Am. Soc. Mass Spectrom.* **1993**, *4*, 117.
(26) Pine, S. H. *Organic Chemistry*, 5th ed.; McGraw-Hill: Singapore, 1987.
(27) Bourissou, D.; Guerret, O.; Gabbai, F. P.; Bertrand, G. *Chem. Rev.* **2000**, *100*, 39.
(28) Hunter, E. P. L.; Lias, S. G. *J. Phys. Chem. Ref. Data* **1998**, *27*, 413.
(29) Stringer, M. B.; Underwood, D. J.; Bowie, J. H.; Allison, C. E.; Donchi, K. F.; Derrick, P. J. *Org. Mass Spectrom.* **1992**, *27*, 270.
(30) Dua, S. K.; Whait, R. B.; Alexander, M. J.; Hayes, R. N.; Lebedev, A. T.; Eichinger, P.-C. H.; Bowie, J. H. *J. Am. Chem. Soc.* **1993**, *115*, 5709.
(31) Derrick, P. J. *Mass Spectrom. Rev.* **1983**, *2*, 285.
(32) Grabowski, J. J.; DePuy, C. H.; Vandoren, J. M.; Bierbaum, V. M. *J. Am. Chem. Soc.* **1985**, *107*, 7384.
(33) Gronert, S.; DePuy, C. H.; Bierbaum, V. M. *J. Am. Chem. Soc.* **1991**, *113*, 4009.
(34) Eberlin, M. N.; Gozzo, F. C. *J. Mass Spectrom.* **2001**, *36*, 1140.
(35) Augusti, R.; Zheng, X. B.; Turowski, M.; Cooks, R. G. *Aust. J. Chem.* **2003**, *56*, 415.
(36) Reynolds, C. H. *J. Am. Chem. Soc.* **1992**, *114*, 8676.
(37) Alvarez, J.; Denault, J. W.; Cooks, R. G. *J. Mass Spectrom.* **2000**, *35*, 1407.
(38) Aue, D. H.; Bowers, M. T. Stabilities of Positive Ions from Equilibrium Gas-Phase Basicity Measurements. In *Gas Phase Ion Chemistry*; Bowers, M. T., Ed.; Academic Press: New York, 1979; Chapter 9.
(39) Robles, E.-S. J.; Chen, P. *J. Phys. Chem.* **1994**, *98*, 6919.
(40) Wang, F.; Ma, S.; Wong, P.; Cooks, R. G.; Gozzo, F. C.; Eberlin, M. N. *Int. J. Mass Spectrom.* **1998**, *179—180*, 195.
(41) Wong, P.-S. H.; Ma, S. G.; Yang, S. S.; Cooks, R. G.; Gozzo, F. C.; Eberlin, M. N. *J. Am. Soc. Mass Spectrom.* **1997**, *8*, 68.
(42) Malow, M.; Penno, M.; Weitzel, K. M. *J. Phys. Chem. A* **2003**, *107*, 10625.
(43) Moon, J. H.; Choe, J. C.; Kim, M. S. *J. Phys. Chem. A* **2000**, *104*, 458.
(44) Smith, B. J.; Hall, N. E. *Chem. Phys. Lett.* **1997**, *279*, 165.
(45) Nicolaides, A.; Radom, L. *J. Am. Chem. Soc.* **1994**, *116*, 9769.
(46) Cone, C.; Dewar, M.-J. S.; Landman, D. *J. Am. Chem. Soc.* **1977**, *99*, 372.
(47) Ausloos, P. *J. Am. Chem. Soc.* **1982**, *104*, 5259.